

# CFD based detection of slamming loads for calibration of a pressure-impulse model

Amin Ghadirian\* and Henrik Bredmose

DTU Wind Energy, Nils Koppels Allé, Building 403, DK-2800 Kgs. Lyngby, Denmark

\*amgh@dtu.dk      hbre@dtu.dk

## 1 Introduction

The calculation of the slamming waves forces is very important in the design process of offshore wind turbine substructures. The currently used methods focus on reproducing the peak and the time series of such forces (cf. Cointe and Armand, 1987 and Wienke and Oumeraci, 2005). Given the stochastic nature of wave breaking, the detailed force time history for even nominally identical waves can show a large variability. The time integral of the force, however, is expected to show a smaller variation. Hence, a pressure-impulse model (PIMP) was presented in Ghadirian and Bredmose, 2019b with only one free parameter that was not determinable from the incident wave,  $\theta_{\max}$ . The model was validated against one CFD generated impact. Its input parameters were obtained from the incident wave and the reference impulse was calculated from the numerical results using a frozen pressure field method. In this study  $\theta_{\max} = \pi/4$  was used in the pressure impulse model. Later the model was validated against impulses calculated by heavy filtering of measured wave forces on a vertical surface-piercing circular cylinder in Ghadirian and Bredmose, 2019a. In the further study of Pierella, Ghadirian, and Bredmose, 2019, OceanWave3D was used to re-simulate experiments with irregular waves and provided input to the PIMP model for the waves that gave slamming. The same heavy filtering approach was applied to detect the experimental impulses and a good match was obtained for  $\theta_{\max} = \pi/5$ . Although the match was consistent, this value of  $\theta_{\max}$  rests on the experimental detection method, which we anticipate to provide a systematic under-prediction of the impulses.

Hence, in the present paper, we study further methods for impulse detection in breaking wave impacts. We obtain the input parameters of the PIMP model from OceanWave3D computations while the resulting impulses are compared to results obtained from CFD computations. Two different methods are used for calculating the impulse from the CFD computations to calibrate the free parameter of the model,  $\theta_{\max}$ . The first method is to use the OceanWave3D slender body force while the second method is the simpler truncation method from Ghadirian and Bredmose, 2019b.

## 2 Models and reproduced cases

The PIMP model presented in Ghadirian and Bredmose, 2019b simplifies the problem of wave slamming on a cylinder to a wedge-shaped volume of fluid. The domain limits in the azimuth direction are  $-\theta_{\max} \leq \theta \leq \theta_{\max}$  and it is divided into heights above and below  $z = -\mu H$ . At the time of impact, the upper part approaches the cylinder with velocity  $U$  in the negative  $x$ -direction. At the free boundaries,  $P = 0$  is satisfied. The non-dimensional pressure-impulse depends on the normalized outer radius,  $b/H$ , impact height  $\mu$ , cylinder radius  $a/b$  and the maximum impact angle  $\theta_{\max}$  as shown in (1). The effect of each parameter was investigated by Ghadirian and Bredmose, 2019b.

$$\frac{P}{\rho U H} \left( \frac{r}{H}, \theta, \frac{z}{H} \right) = f \left( \frac{b}{H}, \mu, \frac{a}{b}, \theta_{\max} \right). \quad (1)$$

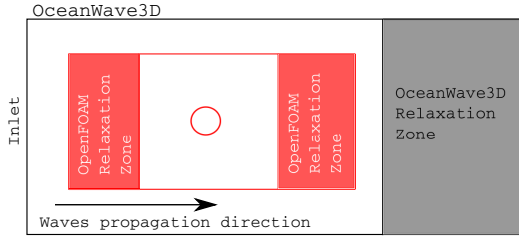


Figure 1: A schematic drawing of the numerical domain of OceanWave3D (grey) and OpenFOAM (red) solvers.

Case	$\alpha$	$H_s$ [m]	$T_p$ [s]
a	1.86	9.5	12
b	1.86	9.5	12
e	2	11	15
c	1.86	9	9
d	2.3	9.5	15

Table 1: The characteristics of the reproduced wave groups in the scale of 50.

Five focus wave groups were reproduced numerically using the OceanWave3D-waves2Foam coupled solver (Paulsen, Bredmose, and Bingham, 2014; Jacobsen, Fuhrman, and Fredsøe, 2012). The potential flow solver, OceanWave3D, uses a simple breaking filter to avoid instability. This filter, becomes active when the vertical particle acceleration gets smaller than half the gravity. The numerical domains of the solvers are shown schematically in figure 1.

The characteristics of the reproduced sea states are shown in table 1 where  $\alpha$  is the scaling factor of the focused wave groups,  $H_s$  is the significant wave height and  $T_p$  is the peak period. The unidirectional waves were chosen to demonstrate different complexity of breaking from simple to evolved breaking. The cylinder diameter was 0.14 cm and the water depth was 0.66 cm.

### 3 Impulse detection in CFD

In the first method for impulse detection, the difference between time integrals of the OpenFOAM and the OceanWave3D inline force time series between two zero-crossings around the slamming peak was calculated and considered to be equal to the impulse only from the slamming phenomenon.

The second method is based on the assumption that slamming of a wave on the cylinder changes the slope of the inline force time series abruptly and the non-slamming part of the wave induces a constant force on the cylinder during the short interval of slamming. Hence, the area of the “hat” on top of the force time history is equal to the impulse of the slamming phenomenon (cf. Ghadirian and Bredmose, 2019b).

In figure 2a to figure 2e the inline force time series of the 5 cases are shown from the OpenFOAM and OceanWave3D computations. The area between the curves and the x-axis are shaded in transparent grey and blue. In plot (a), the OceanWave3D and OpenFOAM results seem very similar. In the latter, however, the slamming can be seen as an abrupt peak around 15 s. Subtracting the blue shaded area from the grey shaded area results in the isolated effect of slamming as intended based on the first method of detecting impulse. This wave included a simple breaking case with no activity in the breaking filter of OceanWave3D. A more evolved breaking can be observed in plot (b) with multiple jets slamming on the cylinder. The OceanWave3D breaking filter was inactive in this case. Similarly, plot (c) and (d) show an evolved breaking wave with multiple jets while the OceanWave3D breaking filter was active. Plots (c), (d) and (e) show larger inconsistency between the OceanWave3D and OpenFOAM results which can be because of the limitations of the breaking filter in OceanWave3D that is merely numerical. In plot (e), the strongest breaking between these cases is shown. In this case, the wave looked entirely different in the OpenFOAM and OceanWave3D domains.

### 4 Comparison to PIMP results

To calculate the corresponding impulses from the PIMP model its input parameters are detected from the wave gauge outputs of the OceanWave3D computations. The fluid thickness,  $H$ , was calculated as

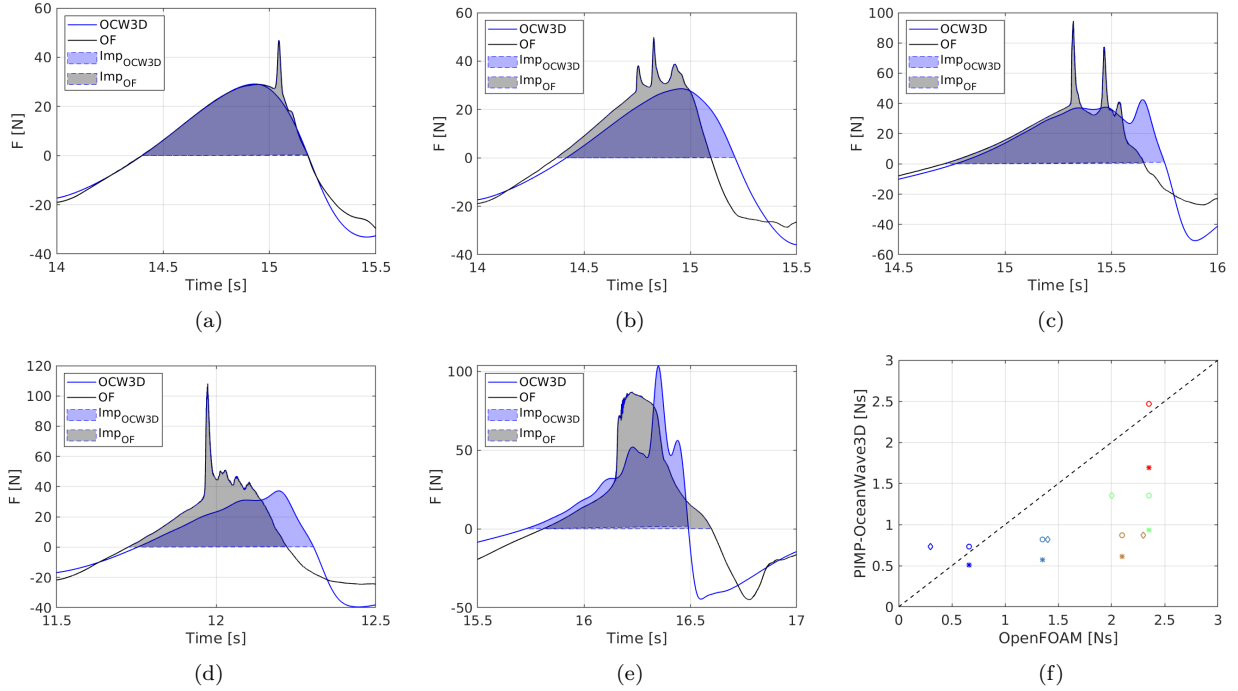


Figure 2: From (a) to (e): Inline force time series from OceanWave3D and waves2Foam (OpenFOAM). The areas under the curves between preceding and following zero-crossing are shaded. The plot letters correspond to the case letters. Plot (f): Comparison of the OpenFOAM and PIMP-OceanWave3D impulses for  $\theta_{\max} = \pi/4$  ( $\circ$ ) and  $\pi/5$  ( $*$ ). The results with truncation impulse detection method are shown by  $\diamond$ . Cases are shown by colors (a), (b), (c), (d) and (e) in this plot.

the depth plus the maximum crest height of the wave and  $a$  is the radius of the cylinder ( $D = 7.0[m]$ ). It was shown in Ghadirian and Bredmose, 2019b that the results of the PIMP model are not sensitive to the outer radius  $b$  when it is larger than an asymptotic value. Hence,  $b$  was chosen to be  $L_p/2$  where  $L_p$  is the peak period wavelength using the linear dispersion relation. Further, as a simple choice, the impact zone height was taken equal to the distance between the still water level and the maximum crest height for the breaking event  $\mu H = \eta_{\max}$ . The impact velocity  $U$ , was calculated from the velocity of the wave crest moving between two adjacent wave gauges in the center and 7 cm upstream from the centre of the cylinder. Two values of  $\pi/5$  and  $\pi/4$  were chosen for  $\theta_{\max}$  and the results were compared between the two sets.

In figure 2f the impulse from the OpenFOAM model and the PIMP model with input variables from OceanWave3D are shown. The results of PIMP-OceanWave3D results with  $\theta_{\max} = \pi/4$  and  $\pi/5$  are shown as a function of the first impulse detection method while the result of PIMP-OceanWave3D with  $\theta_{\max} = \pi/4$  are only plotted as a function of the second impulse detection method. The results from the first case, (a), show very good agreement between the OpenFOAM and the PIMP results with slightly better agreement with  $\theta_{\max} = \pi/4$ . Using the truncation method worsens the agreement. However, this is expected from plot (a) of figure 2 since the slamming part is located on a large slope on the time history and the frozen pressure hypothesis is expected to become invalid. For case b the consistency is slightly lower than the model and CFD results. This inconsistency is most probably because of multiple jets in the breaking wave. The same inconsistency can be seen in cases c and d which also include multiple jets in the breaker. The consistency between the two increases by changing  $\theta_{\max}$  from  $\pi/5$  to  $\pi/4$  which is generally correct for all of the cases. Since the slender body force from OceanWave3D follows the general behaviour of the inline force from OpenFOAM, the impulse calculated using the first method is expected to be reliable. In the third case, c, the

change of the impulse detection method further helps to reduce the inconsistency by reducing the impulse from OpenFOAM. The reason for this is that the two force time series have a slight time shift between them which increases the impulse using the first method. In case d, since the inline force results from OceanWave3D has a skewed but large area underneath, the truncation method worsens the comparison between the PIMP and OpenFOAM results. The strongest breaking wave case, e, gives a surprisingly good agreement between the impulse of the OpenFOAM results, using the first method of impulse detection, and the PIMP model with  $\theta_{\max} = \pi/4$ . From the figure 2, it seems that the good agreement is perhaps incidental, since the wave breaking was very developed in both numerical domains and the difference between the two curves and also the input variables for the PIMP model from OceanWave3D results are not very trustworthy. Using the second method of impulse detection the impulse from the OpenFOAM results is, 9.7 Ns (not presented in the plot for clarity). It should be noted that since the calculation of PIMP-OceanWave3D results is dependant on the wave properties in the OceanWave3D domain, and because of the large differences between the two waves in OpenFOAM and OceanWave3D domains, this inconsistency between the impulse of OpenFOAM and PIMP-OceanWave3D is expected.

In general, the results with  $\theta_{\max} = \pi/4$  show better agreement between the OpenFOAM and the PIMP model results. However, the complexities of the wave breaking makes the calibration of  $\theta_{\max}$  harder. These complexities especially affect the first impulse detection method since they affect the OceanWave3D and OpenFOAM results differently and add to the total uncertainty. The results of PIMP-OceanWave3D will also be improved by improving the breaking filter in OceanWave3D. Nevertheless, these uncertainties are a sign of room for improvement in our calibration method rather than a limitation of the pressure impulse model. Finally, the pressure-impulse formulation is shown to be relatively robust and simple. This gives potential for application in connection to fully nonlinear wave kinematics for improved design calculations as used in this paper together with OceanWave3D.

This work was funded by the Innovation Fund Denmark and other partners as part of DeRisk project with grant number 4106-00038B. This support is gratefully acknowledged by the authors.

## References

- Cointe, R. and J.-L. Armand (1987). “Hydrodynamic Impact Analysis of a Cylinder”. In: *Journal of Offshore Mechanics and Arctic Engineering* 109.3, pp. 237–243.
- Ghadirian, Amin and Henrik Bredmose (2019a). “Initial experimental validation of a pressure impulse model for a vertical circular cylinder”. In: *International Workshop on Water Waves and Floating Bodies*.
- (2019b). “Pressure impulse theory for a slamming wave on a vertical circular cylinder”. In: *Journal of Fluid Mechanics*.
- Jacobsen, Niels Gjøøl, David R Fuhrman, and Jørgen Fredsøe (2012). “A wave generation toolbox for the open-source CFD library: OpenFoam”. In: *International Journal for Numerical Methods in Fluids* 70.9, pp. 1073–1088.
- Paulsen, Bo Terp, Henrik Bredmose, and Harry B. Bingham (2014). “An efficient domain decomposition strategy for wave loads on surface piercing circular cylinders”. In: *Coastal Engineering* 86, pp. 57–76.
- Pierella, Fabio, Amin Ghadirian, and Henrik Bredmose (Nov. 2019). “Extreme Wave Loads on Monopile Substructures: Precomputed Kinematics Coupled With the Pressure Impulse Slamming Load Model”. In: *ASME 2019 2nd International Offshore Wind Technical Conference*. American Society of Mechanical Engineers.
- Wienke, J. and H. Oumeraci (2005). “Breaking wave impact force on a vertical and inclined slender pile - Theoretical and large-scale model investigations”. In: *Coastal Engineering* 52.5, pp. 435–462.